

CFP: Low-overhead Profiling-based Intra-operator Parallelism Generation by Preserving Communication-Free Structures

Weifang Hu¹, Xuanhua Shi¹, Chang Wu¹, Yunkai Zhang¹, Xuan Peng¹, Jiaqi Zhai¹, Hai Jin¹,
Yongluan Zhou², Xuehai Qian³

¹Huazhong University of Science and Technology, ²University of Copenhagen, ³Tsinghua University
{huwf,xhshi,wuchang,m202373843,piecesix,jqzhai,hjin}@hust.edu.cn,zhou@di.ku.dk,xuehaiq@tsinghua.edu.cn

ABSTRACT

This paper introduces *CFP*, a system that search intra-operator parallelism configurations by leveraging runtime profiles of actual parallel programs. The key idea is to profile a *limited* space by identifying a new structure named ParallelBlock, which is a group of operators with the property of communication-free tensor partition propagation: the partition of its input tensor can propagate through all operators to its output tensor without introducing communication or synchronization. Based on this property, an optimal tensor partition of operators within a ParallelBlock should be inferred from the partition of input tensor through partition propagation to prevent the avoidable communication. Thus, the search space can be reduced by only profiling each ParallelBlock with different input tensor partitions at its entry, instead of enumerating all combinations among operators within the ParallelBlock. Moreover, the search space is further reduced by identifying ParallelBlock sequences (segments) with similar parallel behavior. *CFP* computes the overall performance of the model based on the profiles of all segments. On GPT, LLAMA, and MoE models, *CFP* achieves up to a 1.51x, 1.31x, and 3.43x speedup over the state-of-the-art framework, Alpa.

1 INTRODUCTION

Recent advances in large-scale models have propelled remarkable progress in diverse fields [10, 31, 45]. These models, characterized by their extensive parameter sizes and computational requirements, necessitate the collaborative processing power of hundreds or even thousands of GPUs over extended periods. Recent efforts have extended the training of large models to over 10K GPUs [1, 8]. The training has widely adopted a spectrum of parallelism with different communication and computation trade-offs: from coarse-grained or inter-operator parallelism [7, 24, 33] with lower communication intensity between nodes, to tensor or intra-operator parallelism with more intensive communication but also higher computation efficiency within each node. This paper focuses on searching for efficient intra-operator parallelism configurations, which is crucial for the end-to-end performance of large model training [15].

An intra-operator parallelism configuration specifies the partition of each operator across different devices in the computation graph [39], which is ultimately compiled into a single program multiple data (SPMD) form to reduce memory consumption and improve training throughput [43, 47]. However, partitioning every operator in computation graph for achieving optimal parallel efficiency is a NP-hard problem [9]. For intra-operator parallelism, the search space grows exponentially as the number of operators increases [21], making the evaluation of all parallelism configurations

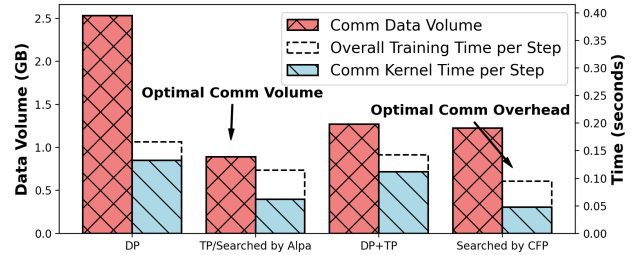


Figure 1: Communication volume and communication kernel overhead of 4 intra-operator parallelism configurations in 2 LLAMA-7B layers on 4 NVIDIA A100-PCIE GPUs, batchsize 64. DP: Data Parallelism, TP: Tensor Parallelism.

in the search space a significant challenge. Despite the promising performance achieved, manually choosing various parallelism settings [14, 25, 49], such as tensor parallelism, data parallelism, or fully sharded data parallelism (FSDP), requires substantial development effort [12].

In the realm of automatic intra-operator parallel frameworks, recent works have introduced many tensor sharding abstractions for operators [29, 38, 43], leading to the construction of comprehensive intra-operator parallel spaces [21, 39, 50]. To tackle the vast search space of intra-operator parallelism, these approaches typically employ efficient search algorithms, such as dynamic programming and integer linear programming to find optimal parallelism configurations within reasonable time [3, 50]. To estimate the performance of the instances in the search space, most approaches [3, 6, 32, 37, 39, 50] leverage the symbolic cost models based on the static information of the computation graph, considering the communication data volume and the FLOPs (Floating Operations) of operations required by the parallelism configuration.

However, this approach suffers from a fundamental drawback: it cannot capture the change of performance characteristics due to downstream compilation and optimizations. One contributing factor is the complex relationship between communication volume and the performance. Fig. 1 highlights the differences in communication volume and per-step training performance among four parallelism configurations for training two hidden layers of the LLAMA2-7B model using XLA framework [28].

We can clearly see that minimizing data communication volume does not necessarily lead to the lowest communication overhead or the best training performance. For a cost model that primarily considers communication volume, such as Alpa [50]’s intra-operator

parallelization cost model, this clearly poses a key challenge. In addition to downstream compilation and optimization, the dynamic selection of communication algorithms and their architecture-dependent implementations also increase performance uncertainty. While it is theoretically possible to include these factors in a symbolic cost model, such a model would be overly complex and impractical.

The approaches based on machine learning [21–23, 30, 40, 52] may capture the complex impacts of performance through establishing the relations among various factors better. However, they suffer from the inadequate modeling of the parallel space and prohibitive search overhead for large models [6].

Methods based on profiling is another option to alleviate the mismatch between estimated performance from cost model and actual performance. Although it has been widely used for searching inter-operator parallel configurations [24, 34, 48], where the entire model or pipeline stage is profiled to determine pipeline partition, applying the profile based methods to the search of intra-operator parallelism configurations is impractical due to the unacceptable overhead of compiling and running each configurations [15]. Aceso [19] built cost models for intra-operator parallelism configurations by separately profiling different types of operators and communication primitives. This method incurs less profiling overhead and can be completed in a reasonable amount of time. However, it still fails to address the mismatch due to downstream compilation and optimization in automatic parallelism involving graph optimizations, such as graph rewriting [36] and kernel fusion [51].

Intuitively, the mismatch is due to certain structures that may be altered through optimizations and the unpredictable communication efficiency. Thus, it is sensible to *fix* the proper parallelism configurations for certain structures that are known to perform well in the computation graph to reduce such effects. On the other hand, this can also reduce the search space. This paper makes the first attempt to explore this approach that “kill two birds with one stone”.

This paper introduces an automatic intra-operator parallel system that selects parallelism configurations using a model segment profile-based cost model. The key idea is to profile a limited space by identifying a new structure named *ParallelBlock*, which is a group of operators enjoying *communication-free tensor partition propagation* property: the partition of its input tensor can propagate through all operators to its output tensor without introducing communication or synchronization. *ParallelBlocks* can be identified by fine-grained data dependencies between tensors in computation graph. Based on this property, an optimal tensor partition of operators within a *ParallelBlock* should be inferred from the partition of input tensor through partition propagation to avoid additional communication. It is because any divergence from the inferred parallelism configurations would incur additional communication. Thus, it is sufficient to profile each *ParallelBlock* with different input tensor partitions at its entry, instead of considering all combinations among operators within the *ParallelBlock*. Essentially, this idea prunes the suboptimal configurations from the intrinsic relation between the model’s sub-structure and intra-operator parallelism configurations, while also reducing profile overhead.

The search space can be further reduced by extracting a set of unique model *segments*, such as multiple identical hidden layers. The segments can be extracted by matching *ParallelBlocks sequences*

and applying fine-grained data dependency graph of tensor contraction operators, ensuring uniform parallel behavior for segments of the same type. The profiles of all model segments are combined to estimate the overall performance, capturing all parallelism configurations within the reduced search space.

Based on *ParallelBlock*, we develop *CFP* (*Communication-Free Preserve*), an automatic parallelization system based on the widely-used XLA compiler. *CFP* has been extensively evaluated across four models in various configurations on two target platforms. It outperforms state-of-the-art automatic intra-operator parallel frameworks, TensorFlow-Alpa, achieving up to 1.51x, 1.31x, and 3.43x speedup on GPT, LLAMA, and MoE models, respectively. The search overhead of *CFP* is independent of the model depth. It can identify optimal parallel configuration for each model in less than 15 minutes.

2 BACKGROUND AND MOTIVATION

2.1 Intra-operator Parallel Space Search

Intra-operator parallelism aims to distribute tensors and computations of each operator in the Data Flow Graph (DFG) across different devices to reduce the memory and computation per device, ultimately generating a SPMD program for the DFG. This parallelization process may incur communication between devices. For instance, when a tensor is partitioned on a dimension that will be reduced, inter-device communication must be conducted to ensure that each device has all necessary data to perform the following computation.

The intra-operator parallel space can be formed by combining parallel templates and parallelism configuration, such as using a combination of data and tensor parallelism for a transformer layer to obtain an intra-operator parallel configuration. Jointly, selecting a partition for each operator leads to a comprehensive but huge intra-operator parallelism search space. For each operator, the partition can be performed in multiple possible dimensions, e.g., matrix multiplication can be split across two different devices in three dimensions, as illustrated in Fig.2(a).

To reduce the variety of operators to be considered, automatic parallel frameworks designate a set of parallel strategies for each type of primitive. The parallel strategies of each fine-grained operator in the compiler intermediate representation (IR) are then combined to construct a search space. The state-of-the-art search algorithms, such as symbolic cost model based dynamic programming and linear programming, produce decent results with reasonable time. Communication overhead, typically measured by the number of communicated bytes derived from the shape and datatype of the communicated data, plays a crucial role in affecting distributed training performance.

2.2 Theoretical vs. Actual Overheads

In practice, there is a substantial gap between the theoretical cost estimated by the cost model and the actual performance produced during actual execution. It is because: (1) multiple layers of code lowering during optimizations when translating parallel configurations into final SPMD parallel programs with communication kernels; and (2) the dynamic selection of communication algorithms:

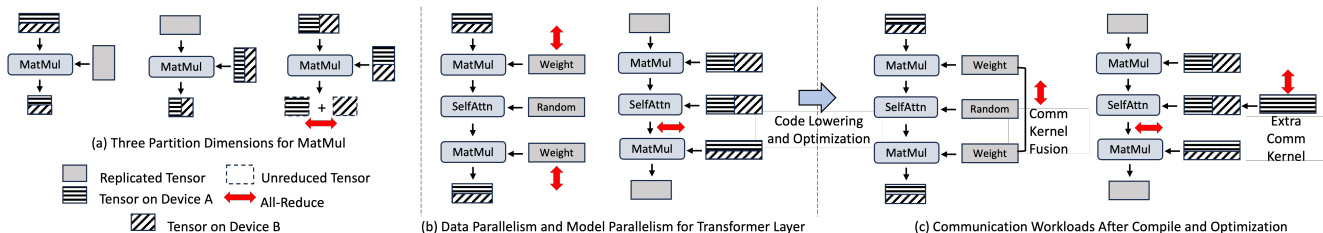


Figure 2: Parallel strategies for MatMul and two parallelism configurations for a Transformer layer. After code lowering and optimizations, there is a noticeable mismatch between the actual communication workloads and the theoretical cost.

their intricate implementations create a complex non-linear relationship between transferred data size and communication time. It is impractical to consider all factors into the code model since it will make the model over-complex and further prolong the search time.

Consider data and tensor parallelism from Megatron-LM [25] for the transformer layer in Fig.2(b). We calculate the communication volume assuming $hidden_size$ is 5120, seq_len is 1024, and $batch_size$ is 16. For data parallelism, each parameter requires All-Reduce on all devices after updates, thus the communication volume is $4 * 4 * hidden_size * hidden_size = 400MB$. For tensor parallelism, the output of the $SelfAttn$ must be reduced before it can be used by the second matrix multiplication operator. Therefore, the theoretical communication volume for tensor parallelism is $4 * batch_size * seq_len * hidden_size = 312.5MB$.

The actual communication overhead diverges significantly from the theoretical communication volume. For tensor parallelism, even with a smaller theoretical communication volume, the actual communication overhead of the parallel program doubles after being compiled by the XLA compiler backend. It is due to the compiler’s restriction that allows RNG operators to run on only one GPU, leading to an All-Reduce operation to distribute random data for dropout operator to other GPUs. For data parallelism, in contrast, the communication efficiency is improved: multiple parameters are synchronized and aggregated to a single large tensor, which can be communicated using a single All-Reduce kernel with higher efficiency. The impact on actual communication overhead is confirmed on 4 A100-PCIe GPUs: the communication time of data parallelism is only 60% of that of tensor parallelism.

2.3 Challenges of Profile-based Approaches

Compiling all parallelism configurations in the intra-operator parallel space and profiling them can alleviate this discrepancy, but it incurs unacceptable time overheads for two reasons:

Exponential growth of the parallel space. For generality, automatic parallel frameworks must construct parallel spaces and perform configuration searches at the compiler IR level. It involves combining multiple parallel strategies for every fine-grained primitive in the computation graph, leading to an *exponential* growth of the parallel space with the model depth. Considering just two GPT hidden layers, they are translated by the XLA compiler into over 1k fine-grained operators, each with multiple parallel strategies. However, such generality is likely overkill: intuitively, designing parallel tensor configurations for a model only requires focusing

on a few key operators. For example, in Megatron-LM [25], parallel strategies are selected for several matrix multiplication operators in the Transformer and reused across all layers. Thus, a practical approach should be able to distinguish the key operators.

Significant profiling overhead. Profiling a candidate configuration involves compiling it into a parallel program and executing it multiple times. The compilation time depends on the complexity of the model structure, with deeper models requiring longer compilation times. The execution time depends on the number of model executions and the computational workloads, which is influenced by factors such as training settings and the efficiency of the configuration.

2.4 Motivation: Profiling Local Structures

To overcome the two challenges, we ask: is it possible to accurately evaluate the parallel strategy combinations for a few key operators (or model blocks) and reuse the evaluation results across each homogeneous model layer? The paper proposes ParallelBlock as the novel local structure to achieve this goal. Specifically, ParallelBlock reduces the profiling overhead from once per combination of partition strategies of all operators in a ParallelBlock, to once per partition strategy of the ParallelBlock’s input tensor.

Fig.3 shows the system overview of *CFP*. It uses data dependency analysis to identify inherent coarser-grained parallel tasks in computation graph, and groups these fine-grained operators into ParallelBlocks. It then constructs the parallel space by combining the parallel strategies of these ParallelBlocks instead of fine-grained primitives inside ParallelBlocks. To capture larger structure and further reduce profiling overhead, it uses sequence matching on ParallelBlocks to identify model *segments* with same parallel spaces and communication behaviors in the computation graph. It then profiles the sub-parallel space of these segments, which is built by combining the parallel strategies of several ParallelBlock inside them. To ensure accuracy, it also profiles the tensor resharding costs between segments. These profiles are reused for each segment in the computation graph and tensor synchronization between segments, and combined to determine the overall execution cost of each instance of the global parallel search space. Finally, the system searches for the most cost-effective parallelism configuration under memory usage limit.

3 PARALLELBLOCK CONSTRUCTION

CFP groups fine-grained operators in the computation graph into multiple ParallelBlocks. All operations within a ParallelBlock need

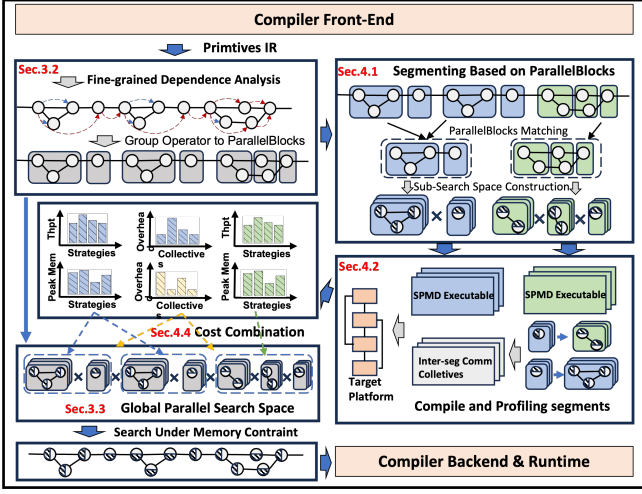


Figure 3: System Overview

to maintain consistent parallel dimensions determined by the partition of its input tensor.

3.1 ParallelBlock: Definition and Property

Existing models inherently contains many coarse-grained structures, where the parallelism of input tensors can be propagated seamlessly to output tensors, e.g., continuous elemental-wise operators. These structures, when translated into fine-grained operators, form *parallelism-preserving subgraphs* on the computation graph. A typical example is the self-attention block in the Transformer, as illustrated in Fig.4(a). Since two *BatchedMatMul* operators only perform partial reduction on the input tensors, each element in the output tensor Y depends on corresponding block regions of the input tensors Q , K , and V , as shown in Fig.4(b). As long as B and H can be evenly divide by the parallelism degree of the target platform, the parallelism of each data dimension on the input tensors can be propagated to the output tensor seamlessly. This makes it possible to treat a subgraph as a whole operator with only two candidate partition dimensions, as shown in Fig.4(c).

Definition. A *ParallelBlock* is formed by grouping parallelism-preserving subgraphs into tensor contraction operators, considered as the basic unit for building parallel space in *CFP*. All operators partition dimension within this subgraph should be inferred from the partition dimension of the first tensor contraction operator of the *ParallelBlock*.

Property: Preserving Communication-Free Structures. For a *ParallelBlock*, the partition of the input tensor can always propagate seamlessly to the output tensors of the *ParallelBlock* *without triggering any data synchronization or communication*. It implies that the optimal parallelism configurations should be selected from the smaller space of the inferred parallelism configuration for all operators inside the *ParallelBlock*. Moreover, maintaining consistent partitions across all operators within the *ParallelBlock* also forms a closure, which does not introduce any side effects in the global parallelization. By sticking to the consistent configurations, we can avoid exploring suboptimal combinations of partition strategies

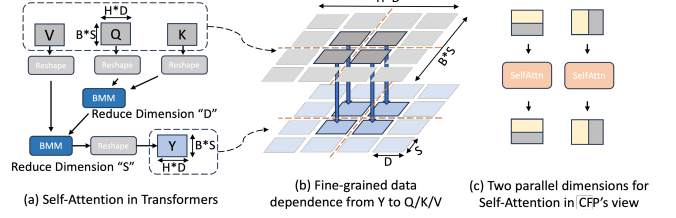


Figure 4: The simplified computation graph of the Self-Attention structure in Transformer is parallelism-preserving. B , S , H , and D represent *batchsize*, *seq_len*, *head_num*, and the *hidden_size* of each head, respectively. BMM refers to *Batched Matrix Multiplication*.

for operators within the *ParallelBlock*, significantly reducing the parallel space, as many of these strategies would lead to redundant data synchronization.

3.2 Dependency Propagation

To precisely identify the parallelism-preserving subgraphs of primitive operators, we model the fine-grained data dependencies between tensors using affine expressions. The data dependency from a tensor $Y[A_0, A_1, \dots, A_N]$ to an another tensor $X[B_0, B_1, \dots, B_N]$ can be represented as:

$$Y(a_0, a_1, \dots, a_{n-1}) \rightarrow X(b_0, b_1, \dots, b_{m-1}),$$

$$b_i = \sum_{j=0}^{n-1} k_j a_j + C, \quad 0 < i < m - 1 \quad (1)$$

where k_j is the coefficient of the affine mapping on j th dimension. In other words, the indices of the dependent element in X can be computed through an affine transformation of the indices of the element in Y .

A subgraph can be regarded as a parallelism-preserving subgraph if there exists a set of positive integers (d_0, d_1, \dots, d_N) , such that the affine mapping between any input tensor X and any output tensor Y in the subgraph satisfy:

$$b_i = \lfloor \frac{a_i}{d_i} \rfloor d_i + k, \quad 0 \leq k < d_i, \quad \frac{A_i}{d_i} \bmod P = 0 \quad (2)$$

where P represents the parallelism degree of target devices, A_i represents the i th dimension size of tensor Y . This dependency implies that parallelism-preserving subgraphs can be evenly distributed along any input tensor data dimension across P devices and executed independently.

Constructing and Propagating Dependency *CFP* constructs fine-grained dependency by first building an identity transformation expression for an initial tensor. It then builds affine expressions for subsequent operators, composing each operator's affine expressions with the previous ones to propagate data dependencies.

The element-wise operator dependency between output and input tensor can be simply expressed as an identity affine transformation. While other operators may add or reduce tensor dimensions, we construct their affine transformations based on their dimension specifications. Table.1 presents the affine transformation expressions constructed by *CFP* for different type of operators. For

Table 1: Affine expressions for different type of operators. Where K represents the interval for splitting dimensions in Reshape operations, and “*” denotes any data point along the dimension. Tensor prefixes and irrelevant dimensions are omitted for simplicity in affine expressions.

Type of Op	Dimension Specifications	Affine Expression
Elem-wise	/	$(a_0, a_1, \dots, a_n) \rightarrow (a_0, a_1, \dots, a_n)$
Reshape	Split dimension i to j, k .	$(\dots, a_j, a_k, \dots) \rightarrow (\dots, K a_j + a_k, \dots)$
Reshape	Merge dimensions i, j to k .	$(\dots, a_k, \dots) \rightarrow (\dots, \lfloor a_k / K \rfloor, a_k \% K, \dots)$
Transpose	Target dimensions: i_0, i_1, \dots, i_n	$(a_0, a_1, \dots, a_n) \rightarrow (a_{i_0}, a_{i_1}, \dots, a_{i_n})$
Broadcast	Add dimensions i	$(\dots, a_i, \dots) \rightarrow (\dots, *, \dots)$
Contraction	Contraction dimension i	$(\dots, a_{i-1}, a_{i+1}, \dots) \rightarrow (\dots, a_{i-1}, *, a_{i+1}, \dots)$

example, the fine-grained data dependency from tensor Y to tensor V in Fig.4

$$Y(i_0, i_1) \rightarrow V(\lfloor \frac{i_0}{S} \rfloor S + s, i_1) : 0 \leq s < S \quad (3)$$

can be derived by composing the following affine expressions.

$$I_R(i_0, i_1, i_2, i_3) \rightarrow V(S i_0 + i_2, D i_1 + i_3) \quad (4)$$

$$I_M(i_0, i_1, i_2, i_3) \rightarrow I_R(i_0, i_1, *, i_3) \quad (5)$$

$$Y(i_0, i_1) \rightarrow I_M(\lfloor i_0 / S \rfloor, \lfloor i_1 / D \rfloor, i_0 \% S, i_1 \% D) \quad (6)$$

where S and D represent the sequence length and hidden size.

Grouping Operators into ParallelBlocks Starting from the output tensors of each tensor contraction operator, *CFP* employs a depth-first search approach to group as many operators as possible, as illustrated in Algorithm 1. For each tensor contraction operator, *DFSAndGroup* starts searching from their output tensors to find the largest parallelism-preserving subgraph and groups them with the tensor contraction operator into ParallelBlocks. Tensor contraction operators are first sorted based on the depth in computation graph. This allows some of them to be grouped into previous ParallelBlock early, thereby avoiding revisiting paths that have already been traversed. The *DFSAndGroup* function checks whether the user’s output tensor satisfies the criteria outlined in Eq.2, and recursively traverses the user’s users on the DFG (*GetAllUsers()*) in a depth-first manner. The traversal process terminates when there are no subsequent operators, or when the data dependencies along the traversal path do not satisfy the parallel-preserving conditions.

Moreover, we group backward operators into the same ParallelBlocks as their corresponding forward operators. This is because they share the same partitioned tensors, such as intermediate results stored in memory. Keeping consistent parallel data dimensions with the forward operators can avoid redundant data synchronization.

3.3 Configuration Construction

To generate an intra-operator parallelism configuration, each operator should be assigned a parallel strategy. *CFP* first selects parallel strategies for the first tensor contraction operator of each ParallelBlock, and then automatically infers the partition dimensions for the other operators. For operators within the ParallelBlocks, their parallel dimensions only need to be consistent with the first tensor contraction operator. As shown in Fig.5(a) to 5(b), the parallel dimensions of the operators within the two ParallelBlocks can

Algorithm 1: DFS for Constructing ParallelBlock.

```

Input : Computation Graph  $G$ 
Output : ParallelBlocks  $PBS$ : Lists of operators
1 Function BuildParallelBlocks( $G$ ):
2    $PBS = \{ \}$ ;
3    $S = \text{SortTensorContractionOpSet}(G)$ ;
4   for each  $s$  in  $S$  do
5      $PB = \{ \}$ ;
6     if  $\text{IsGrouped}(s)$  then
7        $\text{continue}$ ;
8     else
9       Add  $s$  to  $PB$ ;
10       $\text{DFSAndGroup}(s, PB)$ ;
11       $\text{SetGrouped}(PB)$ ;
12    Add  $PB$  to  $PBS$ ;
13  return  $PBS$ ;

14 Function  $\text{DFSAndGroup}(op, PB)$ :
15   $users = \text{GetAllUsers}(op)$ ;
16  for each  $user$  in  $users$  do
17    if  $\text{IsGrouped}(user)$  then
18       $\text{continue}$ ;
19    else
20      if  $\text{Check user, PB with Eq.(2)}$  then
21        Add  $user$  to  $PB$ ;
22        return  $\text{DFSAndGroup}(user, PB)$ ;
23  return;

```

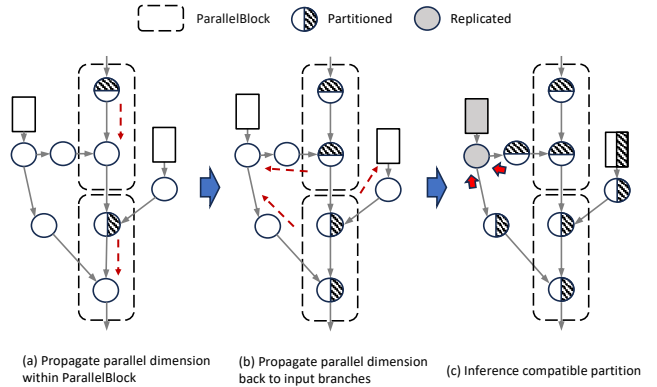


Figure 5: Inferring parallelism configuration for a given parallel dimension for each ParallelBlock.

be derived by propagating the parallel dimensions of the tensor contraction operator.

Some operators are not grouped into ParallelBlocks because they are not on the dominant path of tensor contraction operators. Most of them appear on input branches caused by model parameters. *CFP* finds the operator within the ParallelBlock that receives this input branch and propagates the operator’s parallel dimensions back to the input branch. In Fig.5(b), the parallel dimensions of the right

side parameter are determined based on the parallel dimensions of the first operator in the second ParallelBlock.

In addition, some operators may generate tensors used by multiple ParallelBlocks, and the parallel dimension requirements of different ParallelBlocks for these operators may conflict. This makes their parallel strategies cannot be easily inferred from a single ParallelBlock. *CFP* identifies the data dependency paths from these operators to all related ParallelBlocks and determines compatible parallel strategies for them, as shown in Fig. 5(c).

CFP builds the intra-operator parallel space by combining the parallel strategies of the first tensor contraction operator in all ParallelBlocks and constructs a parallel configuration for each instance within it. The intra-operator parallel space is reduced to a combination of parallel strategies for a few key operators instead of all fine-grained primitives. The size of parallel space depends on the number of ParallelBlocks and the number of partition strategies for the first tensor contraction operator in each ParallelBlock. For a part of the model with N ParallelBlocks and D_i partition strategies for the i -th ParallelBlock, the size of the parallelism configuration search space is $S = \prod_{i=1}^N D_i$.

4 PROFILING MODEL SEGMENTS

By constructing a coarser-grained parallel unit, ParallelBlock, we create a parallel space that depends on the number of ParallelBlocks and the parallel data dimensions of each ParallelBlock. Using profiling to evaluate the parallel space of a model segment, such as one hidden layer, is feasible because it typically has only a few key tensor contraction operators. However, as the number of layers increases, there will still be a considerable number of ParallelBlocks, leading to an expansion of the search space and significant profiling strength. Additionally, since profiling requires multiple runs of the parallel program, the increased model depth also results in longer run times for every profiling step, further increasing the profiling strength. To further reduce profile-based search overhead, this section introduces the notion of model segments that can generate larger unit for profiling. *CFP* leverages *similarities* in model structure to extract a set of unique segments, profiles them separately, and combines the profiles to get the overall cost of a configuration.

4.1 Segment Generation

CFP identify segments in the computation graph that share the same parallel space and exhibit similar parallel execution behaviors under a uniform parallel configuration. These segments are classified as a unique model segments, and their profiles can be reused. The entire model can be reconstructed with the extracted unique segments with *compactness*: the system can generate as few segments as possible, and perform profiling on the more feasible parallel space for each segment.

A straightforward method to identify segments is to use consistent layers defined at the compiler front-end. However, these layer definitions may not always produce identical dataflow graphs during compilation. Variations in data dependencies can prevent them from achieving the same communication behaviors under the same configuration. Another approach is to directly search for identical dataflow subgraphs in the computation graph. However, this method not only incurs significant search overhead but may

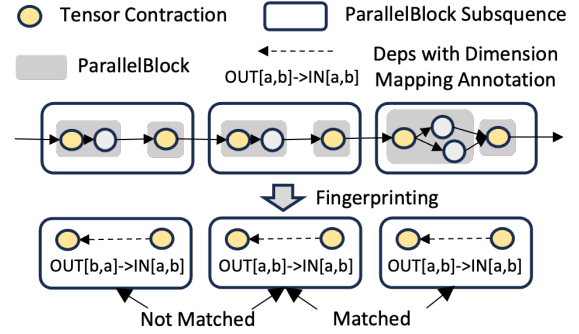


Figure 6: Identify unique model segments based on ParallelBlock subsequences using fine-grained dependencies of tensor contraction operators as fingerprints.

also fail to match segments with the same parallel behavior due to minor differences in trivial operators such as data reorganization.

Thanks to the ParallelBlock-based modeling of parallel space, the computation graph can be represented as a sequence of ParallelBlocks in terms of intra-operator parallelization. Any two model segments must have aligned ParallelBlock sequences to have the same parallel space and similar parallel execution behavior. We thus transform the extraction of unique segments into a pattern matching problem on the sequence of ParallelBlocks. *CFP* uses a simple greedy search algorithm to find a set of subsequences that can cover the original ParallelBlock sequence, while keep the number of unique subsequences as low as possible.

Comparing ParallelBlock sequences is complex because it is essentially a computation subgraph with fine-grained operators. Moreover, the consistency of operators in two ParallelBlock sequences does not reflect whether they have similar parallel execution behavior under same configurations. *CFP* extracts the fine-grained data dependency graph of tensor contraction operators from ParallelBlock subsequences as *fingerprints*, which can significantly reduce matching complexity while ensuring the similarity of parallel execution behavior in matched ParallelBlock subsequences.

Fig.6 shows a simple ParallelBlock sequence containing three subsequences, each with two ParallelBlocks. The fine-grained data dependency graph of tensor contraction operators in each subsequence is extracted to serve as a fingerprint for comparison. The first two subsequences do not match because, despite having the same operators within the ParallelBlocks, differences in dependencies between tensor contraction operators cause inconsistent communication behavior when both subsequences use the same parallel configuration, such as extra communication to reshard the intermediate tensor.

However, the last two subsequences share the same fingerprints, ensuring that they have consistent parallel space and similar communication behavior under same parallel strategies. The fingerprinting method does not require the data flow graphs of segments to be exactly the same. This is because the fingerprint ensures the consistency of tensor contraction operators between segments, while the computational overhead of other types of operators is negligible.

4.2 Profiling Mechanism

CFP first combines all ParallelBlocks’ strategies to construct a sub-search space for a unique segment. It then profiles the communication and computation overhead for each parallel configuration in the sub-search space. Profiling communication overhead is essential because the intensity of communication varies significantly under different parallel configurations. Computation overhead is profiled for two reasons: (1) different communication patterns can lead to extra data movement, such as data splitting and concatenation; and (2) different ways of partitioning operators can affect compilation, memory optimization, and device utilization of computation kernels in accelerate libraries such as CUBLAS.

Directly combining the profiled overhead of all segments does not accurately reflect the total overhead of global parallel configuration, because the mismatched tensor partitioning between segments can lead to additional tensor resharding costs. Therefore, we also profile the tensor resharding overhead between unique segments with dependent tensors. For example, if a model contains two unique segments A and B, we need to combine the parallel configuration for A and B and profile the tensor resharding overhead for up to four combinations: A-A, A-B, B-A, and B-B.

Instead of exhaustively enumerating and profiling every dependent segment pair under different parallel configurations, we pinpoint the source and destination of cross-segment dependencies to specific ParallelBlocks. In this way, we can profile the tensor resharding overhead by combining the different parallel strategies of only two ParallelBlocks. Meanwhile, cross-segment dependencies usually only involve the input tensor of the second segment and the output tensor of the first segment. Therefore, the profiling overhead for tensor resharding overhead between segments is much lower than that for individual segments.

Overall, *CFP* construct two parts of profiles for all unique segment: (1) communication kernel time T_C , computational kernel time T_P , and peak memory consumption M under different parallel configurations of every unique segment; (2) communication kernel time for tensor resharding between connected unique segments, T_R , generated under the combinations of their parallel configurations.

4.3 Profiling Overhead Analysis

The complexity of the proposed profiling method depends on the similarity between different segments and the extent of parallelism-preserving subgraphs within each segment. Assume that a model has M ParallelBlocks and N unique segments, the i -th unique segment contains K_i ParallelBlocks, and the j -th ParallelBlock has $S_{i,j}$ parallel strategies. We model the number of parallel programs that need to be compiled and profiled as follows:

$$\sum_{i=1}^N \left(\prod_{j=1}^{K_i} S_{i,j} + \sum_{(l,k) \in D_{i,j}} S_{i,j} * S_{l,k} \right) \quad (7)$$

where $D_{i,j}$ is a list containing pairs of index of ParallelBlocks that have cross-segment tensor dependencies with ParallelBlock i, j . The left side of the summation represents the number of parallel configuration combinations for all ParallelBlocks within a segment, while the right side represents the number of parallel strategy combinations for ParallelBlock pairs with tensor dependencies across segments.

In the worst case, where the entire model acts as a single unique segment, the number of programs that need to be compiled and profiled is $\prod_{i=1}^M S_i$, which is the simple combination of the parallel strategies of M ParallelBlocks, as explained in Section 3.3. In the best case, where the model consists of a single unique segment repeated, and the cross-segment tensor dependencies only occur between the first and last ParallelBlock within it, the number of programs requiring compilation and profiling is $\prod_{i=1}^K S_i + S_1 * S_K$, i.e., profiling overhead is the sum of all parallel strategies for the K ParallelBlocks within a single segment, plus the resharding cost from the last ParallelBlock to the first ParallelBlock.

Thanks to the extensive use of repeated model structures and wide range of parallelism-preserving subgraphs in existing models, the number of unique segments and the ParallelBlocks in each segment are kept within a reasonable range. For example, after combining two batched matrix multiplications into a ParallelBlock, a transformer layer has only four matrix multiplication operators, corresponding to 4 ParallelBlocks. As a result, our profile-based approach can combine the costs of each parallel configurations by profiling just a few hundred short parallel programs.

CFP leverage the compiler backend to generate SPMD programs for all parallel configurations of each unique segment and all inter-segment resharding. Subsequently, it profiles these programs by running multiple times. Running these programs multiple times incurs a significant time overhead, which depends on the training workload and the efficiency of the parallel configurations. While the backend compilation time for parallel programs can also be substantial, especially when the computation graph is long but the model’s training workload is small. To reduce the search overhead, *CFP* adopts a dynamic profiling time limit, which is updated based on the best results from existing profiles to avoid excessive profiling of inefficient or stalled parallel configurations. It further compiles programs in the profiling space in parallel and overlaps the backend compilation process with the profiling process.

4.4 Cost Model

The overall cost of a global parallel configuration is generated by reusing the profiles of unique segments. Given a model contains N model segments, the n -th segment selects the i_n -th parallel configuration in it’s sub-search space. The cost of overall parallel configuration can be represented as $C_T(i_1, i_2, \dots, i_n, \dots, i_N)$. We use $T_C[n][i]$ represent the communication overhead of n -th unique segments with it’s i -th parallel configuration. The representation of computational cost T_P and memory consumption C_M are similar. For tensor resharding overhead between n -th and its subsequent segment, we represent it with $T_R[n][i][j]$ for the i -th configuration of first segment and the j -th configuration of the second. We define the cost C_T of parallel configuration $(i_0, i_1, \dots, i_{N-1})$ and memory consumption as:

$$C_T = \sum_{n=1}^N (T_C[n][i_n] + T_P[n][i_n]) + \sum_{n=2}^N T_R[n][i_{n-1}][i_n] \quad (8)$$

$$C_M = \sum_{n=1}^N (M[n][i_n]) \quad (9)$$

The first part of the cost is the sum of the computation and communication cost for all model segments, and the second is the sum of the tensor resharding cost between all model segments. Each part of the cost calculation is extracted from the profile of unique segments, ultimately combining to represent the overall cost of a particular global parallel configuration.

After modeling the parallelization cost for every parallelism configuration in the overall parallel space with segments profiles, *CFP* then searches the minimal cost C_T under the constraint of maximum memory usage. Note that this segment-based cost combination method not only allows reusing segment costs to reduce profiling strength but also enables flexible use of different configurations for the same type of segments. For multiple fingerprint-matched segments, some of them may use a high-throughput but memory-intensive configuration, while others may use a low-throughput but memory-efficient configuration, maximizing model throughput while staying as close as possible to the memory usage limit.

5 EVALUATION

CFP is an optimization system based on the Alpa compiler. We implemented an optimization pass of the XLA compiler to group primitive operators to ParallelBlocks and extract unique model segments. We also used the XLA compiler backend and runtime for generating and profiling SPMD programs. Our experiment aimed to answer the following questions:

- (1) Does *CFP*'s reduction for parallel space limit its optimization opportunities, i.e., preventing it from achieving competitive performance?
- (2) Can *CFP*'s profile-based cost model predict actual parallel performance more accurately than symbolic cost model?
- (3) How different are the predictions from the symbolic cost model and actual performance, and the causes?
- (4) How much profiling workload is required in *CFP*, and how long does the searching process take?

To answer these questions, we compared *CFP* with three parallel training frameworks: PyTorch (PT), DeepSpeed-Megatron (DS-M), and Tensorflow-Alpa (Alpa). The popular PyTorch employs data parallelism, which can be considered as intra-operator parallelism configurations that split batch dimension for all operators. DeepSpeed-Megatron provides a manually designed parallel framework, which includes both data and tensor parallelism. The tensor parallelism is also a type of intra-operator parallelism configuration, which splits the reduce dimensions for matrix multiplication and uses All-Reduce collectives to synchronize intermediate results.

Alpa is one of the state-of-the-art automatic parallel frameworks that comprehensively considers inter-operator and intra-operator parallelism. Its intra-operator parallel search space contains parallelism configurations equivalent to both data parallelism and tensor parallelism. As Alpa's optimal solution for multi-level parallelism relies on the optimal intra-operator parallelism configuration for each model stage, we extracted its intra-operator parallel framework to compare with *CFP*. We believe that comparing with Alpa is appropriate, as its intra-operator search process has been widely adopted by newer parallel search frameworks, such as nnScaler [18], while also supporting more recent models than other automatic intra-operator parallel frameworks like FlexFlow [21].

5.1 Evaluation Setup

We used four models in the evaluation: BERT [5], GPT [2], GShard MoE [13] and LLAMA-2 [35]. We set the micro batch size from 2 to 32 per GPU and report the average floating-point operations per second (FLOPS). Note that *CFP* can handle other models besides the evaluated because ParallelBlock construction is based on compiler IR (HLO in XLA).

During the profiling of each parallelism configuration for each unique segment, we began by running the SPMD program 5 times for warm-up, followed by 10 additional runs to collect the desired profile items. For the performance evaluation of the selected parallelism configuration, we ran the test program 100 times and report the average. We evaluated *CFP* on two GPU nodes, each with 8 NVIDIA A100 40GB GPUs connected via PCIe. We also evaluated it on a node with 4 NVIDIA V100 16GB GPUs connected via NVLink to validate its optimization in target platform with higher communication bandwidth. On the A100-PCIe platform, all model are trained with TF32 precision, while on the V100-NVLink platform, we use FP16 precision due to memory constraints.

5.2 Training Performance

In all tests, we observed that even though *CFP* significantly reduces the search space of intra-operator parallel configurations, the search space still includes the data parallel configurations used by PyTorch, the tensor parallel configurations used by DeepSpeed-Megatron, and the communication volume-optimal configurations searched by Alpa. However, *CFP* may not select these configurations as they might not achieve the best profile-based cost. Fig. 7 shows the average throughput achieved by four parallel frameworks on two platforms. PyTorch and DeepSpeed-Megatron use fixed parallel templates, making it difficult to achieve optimal throughput across all experimental settings. This limitation is even more significant for models that require more flexible parallel configurations, such as LLAMA and MoE models, leading to larger performance gaps between fixed parallel templates and optimized configurations.

Single A100-PCIe Node. *CFP* achieved an average performance speedup of 1.17x over Alpa with 4 GPUs and 1.63x with 8 GPUs. We observed that *CFP* consistently selected better configurations through actual runtime profiling, while Alpa's communication volume-based cost model lacks awareness of downstream compilation and the efficiency of communication primitives, leading to inaccurate predictions of communication workload and efficiency in many experimental settings and often resulting in suboptimal configurations.

For GPT and LLAMA models, Alpa tends to split intermediate result tensors and use tensor parallelism to minimize communication volume for small batch sizes. This introduces unexpected communication workloads during downstream compilation, offsetting the benefits of minimizing communication volume in many experimental settings. *CFP* selects to split batch dimensions for each operator in these settings, achieving higher communication efficiency after All-Reduce kernel fusion and up to 1.51x and 1.31x speedup over Alpa on GPT and LLAMA, respectively.

For GShard MoE, *CFP* achieved an average performance speedup of 2.13x over Alpa. Although Alpa's parallel configuration has the optimal communication volume, it relies on multiple inefficient

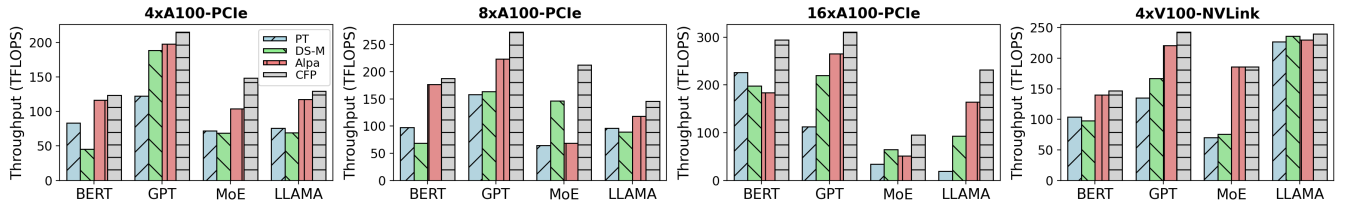


Figure 7: The average training throughput achieved by four parallel frameworks on two platforms.

ncclKernelRecv kernels on PCIe platforms. In contrast, *CFP* uses a hybrid parallel configuration: it splits data dimensions for most operations but splits different dimensions for operators in the expert network, depending on the batch size. These configuration relies on more efficient collective communication primitives like All-Gather and Reduce-Scatter.

Multiple A100-PCIe Node. In experiments with multiple nodes, the parallel configuration can be hierarchical, where one dimension is split on multiple nodes, and another dimension is split on multiple GPUs within each node. We set up the 16 GPUs as 1D and 2D device meshes (1x16, 2x8, 4x4). In this case, the parallel configuration space is greatly expanded, as each operator can either choose to split a single data dimension across 16 GPUs or distribute two data dimensions over the 2D device mesh. We let Alpa search the full space, while *CFP* enforces the batch data dimension be mapped to the outermost level of the device mesh to keep the search space within a reasonable size.

A more complex communication topology makes it harder for Alpa’s cost model to accurately evaluate the performance of different parallel configurations. It struggles to evaluate communication spanning multiple device levels, such as an collective communication involving both inter-node and intra-node. As a result, even though its search space includes both 1D and 2D intra-operator parallel configurations, it overlooks 1D configurations in many cases, even when those could provide better communication efficiency.

Another observation is that multi-level communication provides the compiler with more optimization opportunities, making the actual communication workload differ even more from the theoretical cost. For example, in the MoE model, *CFP* splits the reduction dimension for two matrix multiplication operators in the expert network. This requires using All-Gather and All-Reduce to aggregate data before and after the expert network. In practice, this parallel configuration results in less communication time because the compiler’s downstream optimization rewrites All-Reduce into a more efficient ReduceScatter with smaller communication volume. However, Alpa overlooked this parallel configuration because its estimation of the resharding communication cost was 8 times higher than the actual communication workload. *CFP* avoids these issues by profiling real-world communication costs, achieving an average speedup of 1.51x over Alpa, with maximum speedups of 2.01x on BERT, 1.43x on GPT, 3.06x on MoE, and 1.67x on LLAMA.

Single V100-NVLink Node. With higher GPU communication bandwidth, communication time during training is reduced, resulting in smaller performance differences between configurations. As shown in Fig.7, compared to PyTorch, Deepspeed-Megatron, and Alpa, *CFP* achieved average speedups of 1.73x, 1.61x, and 1.05x. For

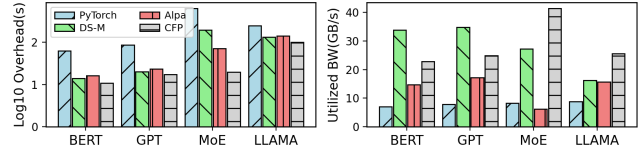


Figure 8: Overhead and achieved bandwidths of communication kernels for four models with batchsizes of 8, 8, 32, and 80, respectively. A logarithmic scale was used for communication overhead.

MoE, both *CFP* and Alpa found parallel configurations that reduced communication time to about 1/20 of the total training time, leading to no significant performance differences. For other models, Alpa still struggles to accurately predict actual communication costs, making the same decisions as on the PCIe platform and failing to achieve optimal performance. In contrast, *CFP* identified optimal configurations based on the profiles from the NVLink platform.

5.3 Communication Overhead Analysis

We observed that most parallel configurations evenly distribute heavy operators across multiple GPUs, making communication overhead the main factor causing significant differences in final throughput, especially on the A100-PCIe platforms. Fig.8 shows the communication overhead and utilized communication bandwidth by the four frameworks on 4xA100-PCIe GPUs. PyTorch data parallel relied on many reduce and scatter operations for parameter updates, which resulted in low utilized communication bandwidth and high communication overhead. Although Deepspeed-Megatron achieved higher utilized communication bandwidth, it relied on predefined parallel templates and failed to optimize communication data volume, leading to suboptimal communication overhead. In contrast, while Alpa always chooses the parallel configuration with the smallest theoretical communication volume, it is not aware of the actual communication load and efficiency, resulting in lower utilized communication bandwidth and higher communication overhead. *CFP* balanced communication volume and efficiency, achieving the smallest communication overhead across the four models.

We further investigated the discrepancy between theoretical cost based on communication volume and real performance on target platform. The theoretical cost was calculated using the same method as Alpa. Fig.9 illustrates the computation and communication kernel overhead for the top 20 parallelism configurations

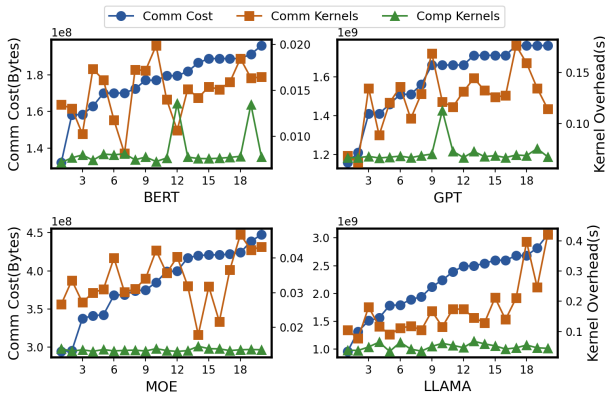


Figure 9: Time of computation and communication kernels for configurations in *CFP*'s intra-operator parallel space. Sorted in ascending order of *Alpa*'s communication volume-based cost, with only the top 20 selected for clarity.

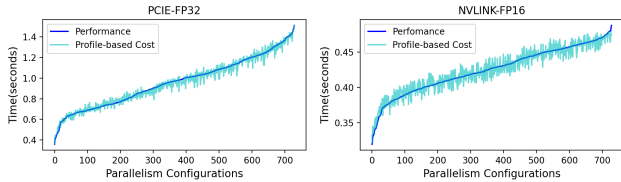


Figure 10: Average training time per iteration and cost predictions by *CFP* for GPT-6.7B with a batchsize of 16.

with minimal theoretical cost in *CFP*'s parallel space. While communication kernel overhead indeed increases with theoretical cost, configurations with similar theoretical cost can have significantly different communication overheads. For instance, in BERT, the 6th to 8th configurations had similar theoretical cost, but their actual overheads differed by a factor of two. Moreover, configurations with optimal communication overhead can have substantially higher theoretical costs, e.g., the configuration (the 14th) with the highest efficiency in MoE had a theoretical cost 1.45 times that of the smallest cost.

We believe two main reasons contribute to such significant discrepancy between cost estimation based on communication volume and actual performance: (1) the unpredictable effects of code lowering and optimization: compiler may generate unexpected communication kernels for certain communication patterns, or it may optimize the communication bandwidth through compiler optimization techniques; and (2) the complex relationship between communication efficiency, target platform, communication algorithms, and tensor shapes: even with similar communication workloads, these factors can significantly affect the communication efficiency, leading to highly variable communication overhead.

CFP's profile-based cost model predicted the performance by combining real-world training profiles. It limited performance unpredictability of parallelism configurations to a small range within the computation graph, i.e., at the connections between model segments. Fig. 10 shows the performance prediction results of *CFP*

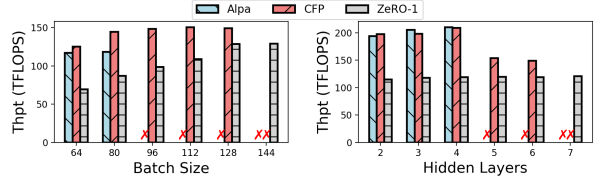


Figure 11: Training performance of LLAMA-7B with different hidden layer numbers and batch sizes. Left: Fixed hidden layer number to 6, increasing batch size. Right: Fixed batch size to 128, increasing hidden layer number.

for the GPT-6.7B model with different configurations on two target platforms. To limit the number of parallel programs, model segments with the same fingerprint were assigned consistent configurations. On the A100-PCIe platform, the root mean square error (RMSE) between the predicted costs and actual training time is 0.03286. On the V100-NVLink platform, the higher utilized communication bandwidth compared to the PCIe platform results in a smaller proportion of cross-segment communication time to total training time, leading to more accurate performance predictions with an RMSE of 0.007885.

5.4 Performance Under Memory Constraints

We evaluated the parallel training throughput of *CFP* under memory constraints on four A100-40GB GPUs. Fig. 11 shows the throughput of different parallel frameworks for training the LLAMA2 model with varying numbers of hidden layers and batch sizes. *Alpa* chose parallelism configurations without integrating memory constraints into the search process, quickly leading to out-of-memory problems as batchsizes and the number of hidden layers increases. *ZeRO* stage-1 distributed all optimizer states across each GPU, minimizing memory usage but suffering from high communication costs, resulting in lower throughput.

CFP balanced throughput and memory usage by selecting different configurations for segments, enabling the training of deeper models than *Alpa* while achieving higher throughput than *ZeRO* stage-1. Note that *CFP* inevitably pruned many memory-efficient configurations, such as fully sharding all tensors, which results in its memory optimization having a lower upper limit compared to *ZeRO*.

5.5 Profile Space and Search Overhead

The profile space depends on the constructed ParallelBlocks and unique model segments, as discussed in Sec.3.3 and Sec.4.2. Besides the embedding and output layers, *CFP* extracted two unique segments from BERT, GPT, and LLAMA: one for the first hidden layer and another for each subsequent hidden layer. Despite having the same structure and tensor shapes, they have different fingerprints due to inconsistent fine-grained dependencies between tensor contraction operators after code lowering. For each segment, it constructed 4 ParallelBlocks, with the first tensor contraction operator (matrix multiplication) in each ParallelBlock having 3 candidate partition dimensions, resulting in $3^4 = 81$ parallel configurations per segment. Tensor resharding across the boundary between the

two segments, from the last ParallelBlock of the first to the first ParallelBlock of the second, requires compiling and profiling $3 * 3 = 9$ groups of communication primitives. Similarly, since the second segment is repeated multiple times, resharding between its first and last ParallelBlock also requires profiling 9 groups of communication primitives. Overall, the profiling space includes $2 * 81 + 2 * 9 = 180$ programs to be compiled and profiled.

For MoE, *CFP* treats the alternating MoE blocks and Transformer blocks as separate segments, constructing 4 ParallelBlocks for each. In MoE blocks, one ParallelBlock’s first tensor contraction operator is a batched matrix multiplication, with the additional batch dimension corresponding to the experts. This adds an extra candidate parallel dimension to this ParallelBlock compared to others, resulting in a slightly larger profile space for the MoE model than other models.

For the profiling space of 2D parallel configurations, we enforce mapping the batch dimension of each ParallelBlock to the node dimension, while GPUs within a single node can parallelize along any data dimension. This restricts the profiling space of 2D parallel configurations to the same size as that of 1D parallel configurations.

CFP’s search overhead can be divided into four parts. *AnalysisPasses*, refers to constructing ParallelBlocks and segmenting model. *ExecCompiling*, represents the overhead of compile and generates all executable programs that need to be profiled. *MetricsProfiling*, refers to the overhead involved in running these programs multiple times to collect profiles. *ComposeSearch*, represents the cost of combining the profiling results of unique segments to search for the globally optimal parallelism configuration.

The magnitude of *ExecCompiling* depends solely on the number of unique segments and the length of each segment. Meanwhile, *MetricsProfiling* is influenced by training workload of each configuration. Fig. 12 shows these two overhead details for GPT-2.6B, MoE-7.1B, and LLAMA-7B with different batch sizes. As the batch size increases, the *ExecCompiling* remains relatively stable, while the cost of *MetricsProfiling* increases. By parallelizing the compilation, overlapping it with the profiling process, and using a dynamic profiling time limit, *CFP* significantly reduced the overall compiling and profiling overhead, as shown by *OptimizedOverall* in Fig. 12.

The overhead of *AnalysisPasses* and *ComposeSearch* is not affected by the training workload but increases as the model depth grows. We evaluated the overhead of them with different numbers of hidden layers on three models, as shown in Fig. 13. In most intra-operator parallelism exploration scenarios (e.g., searching for parallelism configurations inside a pipeline stage), their overhead is much smaller than *ExecCompiling* and *MetricsProfiling*.

5.6 Scalability Analysis

For larger systems with more GPUs, there are two typical cases where *CFP* can be used with no increase of analysis and profiling complexity. (1) Combine *CFP* with data parallelism to exploit multi-dimension intra-operator parallelism. Suppose the model is trained using data parallelism across multiple GPU nodes. *CFP* can be applied in each node using its original workflow, and its profiles can be reused across nodes. (2) Combine *CFP* with pipeline parallelism. *CFP* can explore intra-operator parallelism within each potential

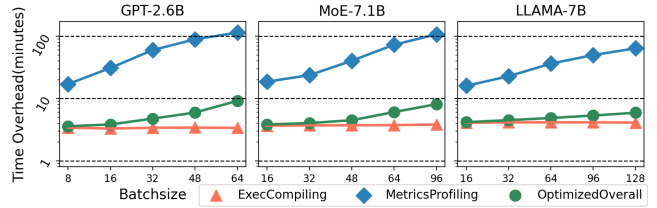


Figure 12: Compiling and profiling time for unique segments in three models on a platform with a 24-core processor and 4 A100-PCIe GPUs.

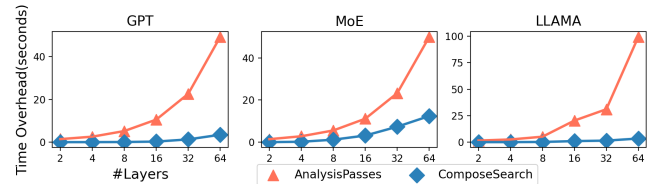


Figure 13: Analyzing and searching time for different number of layers of three models on a platform with a 24-core processor.

pipeline stage, where the profile results of model segments (smaller than a stage) can also be reused for stage profiling.

For larger models, *CFP*’s profiling space will not increase unless there are new unique segments. The increase in the number of layers may raise *CFP*’s analysis overhead (building ParallelBlocks and unique segments), and increasing configuration settings like hidden size may raise the profiling overhead for unique segments. However, these overheads remain negligible compared to the training time.

5.7 Case Study

GShard MoE on A100-PCIe. Fig.??(a)(b) shows the parallel configurations searched by Alpa and *CFP* for a single MoE layer on a single GPU node. Alpa splits the data dimension of each operator and adopts “expert parallelism” for the expert network, assigning different experts to different devices. This requires All-to-All communication to reshare intermediate results before and after the expert network and All-Reduce to aggregate gradients. *CFP* selects different parallel configurations based on the batch size: when the batch size is smaller than 96, it uses tensor parallelism to split the parameters of the expert network. This requires All-Gather to reshare tensors before the expert network and All-Reduce to aggregate results after the expert network, where the All-Reduce operation is rewritten by the compiler into a more efficient Reduce-Scatter with lower communication volume, as shown in Fig.??(b). For larger batch sizes, *CFP* splits the batch data dimension for all operators.

Alpa overlooked this parallel configuration because it failed to foresee the rewriting of communication primitives by the downstream compiler to reduce the communication workload. As a result, it overestimated the communication cost of the tensor resharing after expert network by 8 times compared to the actual communication volume in 16 GPUs training. It also failed to foresee that All-to-All operations would be dispatched to ncclSendRecv kernels,

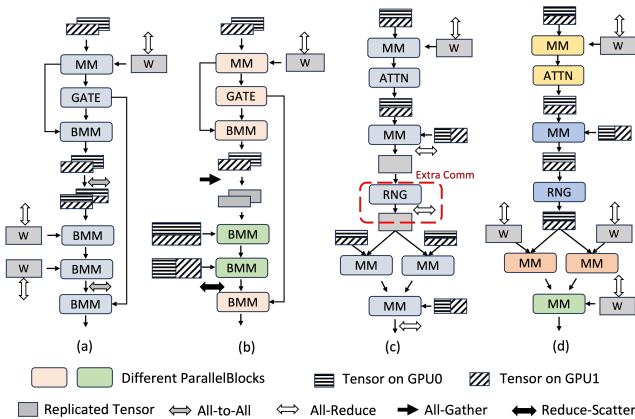


Figure 14: Parallelism configurations searched by Alpa and CFP for MoE-7.1B batchsize 16 on A100-PCIe and LLAMA-7B batchsize 80 on V100-NVLink. GATE, ATTN, and RNG stand for gated network, attention block, and random number generator operator, respectively.

which are highly inefficient on PCIe platforms. We observed that the parallel configurations searched by Alpa incurred twice the communication overhead of *CFP* for batch sizes smaller than 96 and over three times the overhead for larger batch sizes.

LLAMA on V100-NVLink. Fig.??(c)(d) shows the parallel configurations searched by Alpa and *CFP* for LLAMA-7B with a batch size of 80. Alpa splits the batch dimension of input data in the self-attention part and then splits parameters for the remaining operators to minimize communication volume. However, this causes each GPU to call the random number generator operator independently, leading the compiler backend to insert extra AllReduce for random data synchronization. In contrast, *CFP* splits all operators along the batch dimension, merges all parameter gradient synchronizations into a single communication kernel for better efficiency, and avoids extra communication. Moreover, due to the higher interconnect bandwidth between GPUs on the NVLink platform, computation overhead has a more critical impact on overall training time. We observed that frequent communication in Alpa’s parallel configuration introduced more data movement operators (concat and split), making its computation overhead about 10% higher than *CFP*.

6 RELATED WORKS

Modeling the Intra-operator Parallel Space. Many works [27, 43, 46] offer concise yet comprehensive methods to express tensor partitioning, accommodating various parallel paradigms. Parallel strategies that partition temporal dimension for operators have been adopted by recent parallel systems [11, 38, 42, 44] to expand the intra-operator parallel spaces. Some works [4, 16, 26, 41] discussed the scheduling space of after tensor partitioning, which favored overlapping communication and computation to hide communication overhead.

Automatic Search for Intra-operator Parallel Space. To efficiently search for parallelism configurations in the vast intra-operator parallel space, most works, including ToFu [39], TensorOpt [3], PaSE [6], AccPar [32], HAP [47], and PrimPar [38], have employed various symbolic cost models and dynamic programming-based search algorithms. FlexFlow [21] and Automap [30] used Monte Carlo-based search algorithm and employed ML-based approach to evaluate the performance of parallelism configurations. Colossal-Auto [20] uses ILP solver to find the parallelism configuration with lowest communication volume, consistent with Alpa’s intra-operator parallel search method [50]. Aceso [19] builds a cost model for intra-operator parallelism configurations, relying on pre-profiling of each fine-grained operator and communication primitive. It optimize pipeline stage partition with an iterative heuristic strategy, but still relying on parallel configuration templates of Megatron[25] for intra-operator parallelism.

These efforts have designed suitable cost models to closely approximate actual parallel performance, yet there’s still a challenge in avoiding discrepancies between theoretical costs and real-world performance. Our work demonstrates that the tensor parallel space can be reduced to considering only a few ParallelBlocks, thus enabling the use of real runtime metrics as the cost model for selecting parallel configurations.

Combine Intra-operator Parallelism and Pipeline Parallelism. Many frameworks use limited parallelism configurations within each pipeline stage without fully exploring the intra-operator parallel space [7, 24, 34]. Alpa [50] explores intra-operator parallelism and pipeline parallelism in two separate stages and maps them to device layers based on communication characteristics. Aceso [19] combines the exploration of intra-operator parallelism and pipeline parallelism by using reconfiguration mechanisms to alleviate performance bottlenecks. nnScaler [18] provides a set of parallel scheduling abstractions, allowing domain experts to construct flexible search spaces for parallelization plans in any DNN model. Based on the constraints provided by experts, it leverages existing search strategies to explore the reduced search space and generate parallelization plans, i.e., Alpa for intra-operator parallelism and Tessel [17] for pipeline parallelism.

7 LIMITATIONS AND DISCUSSION

Currently, *CFP* has the following limitation:

- (1) It does not consider additional levels of parallelism, such as pipeline parallelism. However, as discussed in Sec.5.6, its segment sub-search space building and profiling method can be easily extended to pipeline parallel frameworks, providing more accurate stage profiles for pipeline partitioning.
- (2) It does not account for multi-granularity overlapping between communication and computation, which increases uncertainty in downstream optimizations and widens the gap between symbolic cost and actual performance. We believe *CFP* remains unaffected as it is based on runtime profiles.

8 CONCLUSION

This paper introduces *CFP*, a system that search intra-operator parallelism configurations by leveraging runtime profiles of actual

parallel programs. The key idea is to profile a limited space by identifying a new structure named ParallelBlock, which is a group of operators enjoying communication-free tensor partition propagation. An optimal tensor partition of operators within a ParallelBlock should be inferred from the partition of input tensor through partition propagation to avoid additional communication. Thus, it is sufficient to profile each ParallelBlock with different input tensor partitions. On GPT, LLAMA, and MoE models, CFP achieves up to a 1.51x, 1.31x, and 3.43x performance improvement over the state-of-the-art framework, Alpa.

REFERENCES

- [1] Meta AI. 2024. Introducing Meta Llama 3: The most capable openly available LLM to date. *Meta AI Blog*. Available at: <https://ai.meta.com/blog/meta-llama-3/>.
- [2] Tom B. Brown, Benjamin Mann, Nick Ryder, Melanie Subbiah, Jared Kaplan, Prafulla Dhariwal, Arvind Neelakantan, Pranav Shyam, Girish Sastry, Amanda Askell, Sandhini Agarwal, Ariel Herbert-Voss, Gretchen Krueger, Tom Henighan, Rewon Child, Aditya Ramesh, Daniel M. Ziegler, Jeffrey Wu, Clemens Winter, Christopher Hesse, Mark Chen, Eric Sigler, Matusz Litwin, Scott Gray, Benjamin Chess, Jack Clark, Christopher Berner, Sam McCandlish, Alec Radford, Ilya Sutskever, and Dario Amodei. 2020. Language Models are Few-Shot Learners. *arXiv:2005.14165* [cs.CL].
- [3] Zhenkun Cai, Xiao Yan, Kaihao Ma, Yidi Wu, Yuzhen Huang, James Cheng, Teng Su, and Fan Yu. 2021. Tensoropt: Exploring the tradeoffs in distributed dnn training with auto-parallelism. *IEEE Transactions on Parallel and Distributed Systems* 33, 8 (2021), 1967–1981.
- [4] Chang Chen, Xiuhong Li, Qianchao Zhu, Jiangfei Duan, Peng Sun, Xingcheng Zhang, and Chao Yang. 2024. Centauri: Enabling Efficient Scheduling for Communication-Computation Overlap in Large Model Training via Communication Partitioning. In *Proceedings of the 29th ACM International Conference on Architectural Support for Programming Languages and Operating Systems, Volume 3* (La Jolla, CA, USA) (ASPLOS '24). Association for Computing Machinery, New York, NY, USA, 178–191. <https://doi.org/10.1145/3620666.3651379>
- [5] Jacob Devlin, Ming-Wei Chang, Kenton Lee, and Kristina Toutanova. 2019. BERT: Pre-training of Deep Bidirectional Transformers for Language Understanding. *arXiv:1810.04805* [cs.CL].
- [6] Venmugil Elango. 2021. Pase: Parallelization Strategies for Efficient DNN Training. In *2021 IEEE International Parallel and Distributed Processing Symposium (IPDPS)*. 1025–1034. <https://doi.org/10.1109/IPDPS49936.2021.00111>
- [7] Yanping Huang, Youlong Cheng, Ankur Bapna, Orhan Firat, Dehao Chen, Mia Chen, HyoukJoong Lee, Jiquan Ngiam, Quoc V Le, Yonghui Wu, et al. 2019. Gpipe: Efficient training of giant neural networks using pipeline parallelism. *Advances in neural information processing systems* 32 (2019).
- [8] Ziheng Jiang, Haibin Lin, Yinmin Zhong, Qi Huang, Yangrui Chen, Zhi Zhang, Yanghua Peng, Xiang Li, Cong Xie, Shibiao Nong, Yulu Jia, Sun He, Hongmin Chen, Zhihao Bai, Qi Hou, Shipeng Yan, Ding Zhou, Yiyao Sheng, Zuo Jiang, Haohan Xu, Haoran Wei, Zhang Zhang, Pengfei Nie, Leqi Zou, Sida Zhao, Liang Xiang, Zherui Liu, Zhe Li, Xiaoying Jia, Jianxi Ye, Xin Jin, and Xin Liu. 2024. MegaScale: Scaling Large Language Model Training to More Than 10,000 GPUs. *arXiv:2402.15627* [cs.LG].
- [9] Ken Kennedy and Ulrich Kremer. 1998. Automatic data layout for distributed-memory machines. *ACM Trans. Program. Lang. Syst.* 20, 4 (jul 1998), 869–916. <https://doi.org/10.1145/291891.291901>
- [10] Alexander Kirillov, Eric Mintun, Nikhila Ravi, Hanzi Mao, Chloe Rolland, Laura Gustafson, Tete Xiao, Spencer Whitehead, Alexander C. Berg, Wan-Yen Lo, Piotr Dollár, and Ross Girshick. 2023. Segment Anything. *arXiv:2304.02643* [cs.CV].
- [11] Martin Kong, Raneem Abu Yosef, Atanas Rountev, and P. Sadayappan. 2023. Automatic Generation of Distributed-Memory Mappings for Tensor Computations. In *Proceedings of the International Conference for High Performance Computing, Networking, Storage and Analysis* (<conf-loc>, <city>Denver</city>, <state>CO</state>, <country>USA</country>, </conf-loc>) (SC '23). Association for Computing Machinery, New York, NY, USA, Article 64, 13 pages. <https://doi.org/10.1145/3581784.3607096>
- [12] Dmitry Lepikhin, HyoukJoong Lee, Yuanzhong Xu, Dehao Chen, Orhan Firat, Yanping Huang, Maxim Krikun, Noam Shazeer, and Zhifeng Chen. 2020. GShard: Scaling Giant Models with Conditional Computation and Automatic Sharding. *arXiv:2006.16668* [cs.CL]. <https://arxiv.org/abs/2006.16668>
- [13] Dmitry Lepikhin, HyoukJoong Lee, Yuanzhong Xu, Dehao Chen, Orhan Firat, Yanping Huang, Maxim Krikun, Noam Shazeer, and Zhifeng Chen. 2021. GShard: Scaling Giant Models with Conditional Computation and Automatic Sharding. In *9th International Conference on Learning Representations, ICLR 2021, Virtual Event, Austria, May 3-7, 2021*. OpenReview.net. <https://openreview.net/forum?id=qrwe7XHTmYb>
- [14] Shen Li, Yanli Zhao, Rohan Varma, Omkar Salpekar, Pieter Noordhuis, Teng Li, Adam Paszke, Jeff Smith, Brian Vaughan, Pritam Damania, et al. 2020. Pytorch distributed: Experiences on accelerating data parallel training. *arXiv preprint arXiv:2006.15704* (2020).
- [15] Peng Liang, Yu Tang, Xiaoda Zhang, Youhui Bai, Teng Su, Zhiqian Lai, Linbo Qiao, and Dongsheng Li. 2023. A Survey on Auto-Parallelism of Large-Scale Deep Learning Training. *IEEE Transactions on Parallel and Distributed Systems* 34, 8 (2023), 2377–2390. <https://doi.org/10.1109/TPDS.2023.3281931>
- [16] Zhiqi Lin, Youshan Miao, Guodong Liu, Xiaoxiang Shi, Quanlu Zhang, Fan Yang, Saeed Maleki, Yi Zhu, Xu Cao, Cheng Li, Mao Yang, Lintao Zhang, and Lidong Zhou. 2023. SuperScaler: Supporting Flexible DNN Parallelization via a Unified Abstraction. *arXiv:2301.08984* [cs.DC]. <https://arxiv.org/abs/2301.08984>
- [17] Zhiqi Lin, Youshan Miao, Guanbin Xu, Cheng Li, Olli Saarikivi, Saeed Maleki, and Fan Yang. 2024. Tessel: Boosting Distributed Execution of Large DNN Models via Flexible Schedule Search. In *2024 IEEE International Symposium on High-Performance Computer Architecture (HPCA)*. 803–816. <https://doi.org/10.1109/HPCA57654.2024.00067>
- [18] Zhiqi Lin, Youshan Miao, Quanlu Zhang, Fan Yang, Yi Zhu, Cheng Li, Saeed Maleki, Xu Cao, Ning Shang, Yilei Yang, Weijiang Xu, Mao Yang, Lintao Zhang, and Lidong Zhou. 2024. nnScaler: Constraint-Guided Parallelization Plan Generation for Deep Learning Training. In *18th USENIX Symposium on Operating Systems Design and Implementation (OSDI 24)*. USENIX Association, Santa Clara, CA, 347–363. <https://www.usenix.org/conference/osdi24/presentation/lin-zhiqi>
- [19] Guodong Liu, Youshan Miao, Zhiqi Lin, Xiaoxiang Shi, Saeed Maleki, Fan Yang, Yungang Bao, and Sa Wang. 2024. Aceso: Efficient Parallel DNN Training through Iterative Bottleneck Alleviation. In *Proceedings of the Nineteenth European Conference on Computer Systems* (<conf-loc>, <city>Athens</city>, <country>Greece</country>, </conf-loc>) (EuroSys '24). Association for Computing Machinery, New York, NY, USA, 163–181. <https://doi.org/10.1145/3627703.3629554>
- [20] Yuliang Liu, Shenggui Li, Jiarui Fang, Yanjun Shao, Boyuan Yao, and Yang You. 2023. Colossal-Auto: Unified Automation of Parallelization and Activation Checkpoint for Large-scale Models. *CoRR, abs/2302.02599* (2023).
- [21] Wenyan Lu, Guihai Yan, Jiajun Li, Shijun Gong, Yinhe Han, and Xiaowei Li. 2017. Flexflow: A flexible dataflow accelerator architecture for convolutional neural networks. In *2017 IEEE International Symposium on High Performance Computer Architecture (HPCA)*. IEEE, 553–564.
- [22] Azalia Mirhoseini, Anna Goldie, Hieu Pham, Benoit Steiner, Quoc V. Le, and Jeff Dean. 2018. A Hierarchical Model for Device Placement. In *6th International Conference on Learning Representations, ICLR 2018, Vancouver, BC, Canada, April 30 - May 3, 2018, Conference Track Proceedings*. <https://openreview.net/forum?id=Hkc-TeZ0W>
- [23] Azalia Mirhoseini, Hieu Pham, Quoc V. Le, Benoit Steiner, Rasmus Larsen, Yuefeng Zhou, Naveen Kumar, Mohammad Norouzi, Samy Bengio, and Jeff Dean. 2017. Device placement optimization with reinforcement learning. In *Proceedings of the 34th International Conference on Machine Learning - Volume 70* (Sydney, NSW, Australia) (ICML '17). JMLR.org, 2430–2439.
- [24] Deepak Narayanan, Aaron Harlap, Amar Phanishayee, Vivek Seshadri, Nikhil R Devanur, Gregory R Ganger, Phillip B Gibbons, and Matei Zaharia. 2019. PipeDream: Generalized pipeline parallelism for DNN training. In *Proceedings of the 27th ACM Symposium on Operating Systems Principles*. 1–15.
- [25] Deepak Narayanan, Mohammad Shoeybi, Jared Casper, Patrick LeGresley, Mostafa Patwary, Vijay Korthikanti, Dmitri Vainbrand, Prithvi Kashinkunti, Julie Bernauer, Bryan Catanzaro, Amar Phanishayee, and Matei Zaharia. 2021. Efficient Large-Scale Language Model Training on GPU Clusters Using Megatron-LM. In *Proceedings of the International Conference for High Performance Computing, Networking, Storage and Analysis* (St. Louis, Missouri) (SC '21). Association for Computing Machinery, New York, NY, USA, Article 58, 15 pages. <https://doi.org/10.1145/3458817.3476209>
- [26] Suchita Pati, Shaizeen Aga, Mahzabeen Islam, Nuwan Jayasena, and Matthew D. Sinclair. 2024. T3: Transparent Tracking & Triggering for Fine-grained Overlap of Compute & Collectives. In *Proceedings of the 29th ACM International Conference on Architectural Support for Programming Languages and Operating Systems, Volume 2* (La Jolla, CA, USA) (ASPLOS '24). Association for Computing Machinery, New York, NY, USA, 1146–1164. <https://doi.org/10.1145/3620665.3640410>
- [27] PyTorch Team. 2023. PyTorch DistributedTensor. *PyTorch Developer Discussion*. Available at: <https://dev-discuss.pytorch.org/t/rfc-pytorch-distributedtensor/740>.
- [28] Amit Sabne. 2020. Xla: Compiling machine learning for peak performance. *Google Res* (2020).
- [29] Keshav Santhanam, Siddharth Krishna, Ryota Tomioka, Andrew Fitzgibbon, and Tim Harris. 2021. Distir: An intermediate representation for optimizing distributed neural networks. In *Proceedings of the 1st Workshop on Machine Learning and Systems*. 15–23.
- [30] Michael Schaarschmidt, Dominik Grewe, Dimitrios Vytiniotis, Adam Paszke, Georg Stefan Schmid, Tamara Norman, James Molloy, Jonathan Godwin, Norman Alexander Rink, Vinod Nair, et al. 2021. Automap: Towards ergonomic automated parallelism for ml models. *arXiv preprint arXiv:2112.02958* (2021).